REACTIVE & FUNCTIONAL POLYMERS

Properties of native and oxidized corn starch/polystyrene blends under conditions of reactive extrusion using zinc octanoate as a catalyst

CrossMark

Tomy J. Gutiérrez *, Vera A. Alvarez

Grupo de Materiales Compuestos de Matriz Polimérica (CoMP), Instituto de Investigaciones en Ciencia y Tecnología de Materiales (INTEMA), Facultad de Ingeniería, Universidad Nacional de Mar del Plata (UNMdP) y Consejo Nacional de Investigaciones Científicas y Técnicas (CONICET), Colón 10850, B7608FLC Mar del Plata, Argentina

ABSTRACT

Native and oxidized corn (*Zea mays*) starch/polystyrene (PS) blends containing glycerol as a plasticizer were prepared by reactive extrusion in a twin-screw extruder using zinc octanoate ($Zn(Oct)_2$) as a catalyst, followed by compression molding. Blends were characterized in terms of their: average molecular weight, moisture content, infrared (FTIR) spectra, water solubility, thermogravimetric (TGA) properties, differential scanning calorimetry (DSC) curves, X-ray diffraction (XDR) patterns, stability in acidic or alkaline medium, and microstructural, mechanical and antimicrobial properties. The results clearly show that the catalyst used produced cross-linking between the starch and PS, and that the oxidative modification of the starch increased its reactivity. This was demonstrated by the increase in molecular weight, thermal resistance, and hydrophobicity of films prepared from the oxidized starch/PS plus catalyst. This increase in hydrophobicity of the starch modified systems was due to the carboxyl and carbonyl groups introduced into the starch structure. As a result, phase separation was more obvious, despite the increase in the cross-linking rate between the oxidized starch and the PS. Finally, none of the films showed signs of swelling or antimicrobial activity. Nonetheless, the catalyst exhibited excellent antimicrobial activity against the pathogenic microorganisms evaluated.

© 2017 Elsevier B.V. All rights reserved.

1. Introduction

Starch-based films have often been proposed as food packaging materials [1]. This is mainly because they are biodegradable thus reducing, at least in part, some of the problems caused by the use of synthetic plastics from the petroleum industry [2,3]. Nevertheless, these materials have some drawbacks such as their hydrophilic nature, which makes them highly sensitive to water [4]. For this reason, several strategies to improve their properties have been proposed in recent years. Among these, the development of films based on starch/polystyrene (PS) blends has enjoyed a growing interest [5,6]. Nevertheless, PS and polysaccharides are thermodynamically immiscible, i.e. they show a lack of polymeric compatibility due to their different polarities. The low affinity of starch-PS materials for each other means that simple blending leads to polymer phase separation with limited adhesion between the polymer interfaces, resulting in films with poor properties that are inadequate as packaging materials [7].

With this in mind several catalysts have been used, under conditions of reactive extrusion (REx), to generate cross-linking reactions within a polymer blend, especially thermoplastic starch (TPS). REx is a process that combines mass and heat transport operations with simultaneous chemical reactions taking place inside the extruder, in order to modify the properties of existing polymers or to create new ones. This process is increasingly being employed as a powerful technique to develop and manufacture a variety of novel polymeric materials in a highly efficient and flexible way. The combination of chemical reactions and transport phenomena in an extruder provides a great window of opportunity for the compatibilization of synthetic resins and biopolymers, such as starch, or the compatibilization of synthetic resins and natural fillers, under current industrial conditions [8].

The use of catalysts in these processes is based on the fact that the temperatures and pressures of processing starch-based biodegradable composites activate the catalyst, thereby producing an increase in the reaction rate, i.e. the kinetics of the cross-linking reaction are favored. In this way, the compatibility of starch-based polymer blends can be improved by a process that is scalable industrially. Some examples of the many different catalysts reported in the literature are: tin(II) bis(2-ethylhexanoate) ($Sn(Oct)_2$), lithium octanoate ($Y(Oct)_3$), aluminum sec-butoxide ($Al(O^{sec}Bu)_3$), aluminum triisopropoxide ($Al(O-^{i}Pr)_3$), sodium hydride (NaH), tributyltin methoxide (nBu_3SnOMe), tetrabutyl titanate ($Ti(OBu)_4$), triphenylphosphine ($P(C_6H_5)_3$), *N*-acetyl

caprolactam, potassium persulfate (K$_2$S$_2$O$_8$), 4-dimethylaminopyridine (DMAP), 2,5-dimethyl-2,5-di-(tert-butylperoxy)hexane (Lupersol 101), tetraethyl orthosilicate (TEOS), dicumyl peroxide (DCP), di-tert-butyl peroxide, benzoyl peroxide, ceric ammonium nitrate (CAN), glyoxal, titaniumn-butoxide, aluminum mono- and trialkoxides [9–32]. However, the use of zinc octanoate (Zn(Oct)$_2$) as a catalyst has not been evaluated under REx conditions. The antimicrobial effects of zinc are well known [33]. Thus, this catalyst could have a potential anti-microbial effect, which would enable the development of food packaging with active properties.

On a different note, most of the studies found in the literature related to starch materials have focused on films obtained by the casting method, and processing methods such as blown extrusion, compression or injection molding are less reported. Solvent casting is the most common method for small-scale biopolymer film preparation, and involves solubilization, casting, and drying steps. Despite this being a good and adequate technique on a laboratory scale, it is considered to be a high energy-consuming procedure.

Procedures for the efficient production of high quality, biodegradable films are thus still required by industry. With this in mind, the scaling-up of processing methods using equipment designed for synthetic polymers is indispensable [34,35]. In this context, extrusion, blowing, injection and thermo-compression are viable alternatives due to their energy efficiency and high productivity [36–38]. In particular, extrusion followed by thermo-compression is useful as a processing method because of its simplicity. These methods could thus be used to provide a feasible way of developing biomaterials that are both economical and environmentally friendly [39].

The aim of our research was to evaluate the effect of adding a catalyst, as well as the possible advantages of oxidized corn starch over native starch. This, due to the fact that modifying the starch would increase the number of susceptible sites where the reactive reaction (cross-linking) with PS using Zn(Oct)$_2$ could occur. Finally, it is worth noting that cross-linking reactions raise the average molecular weight of starch, and also introduce chemical bridges between the different molecules [40]. This increases the thermal resistance of the films, which is very important during the processing of polymers [41]. In addition, these reactions should reduce the high sensitivity of these materials to moisture, as well as enhancing their physicochemical properties [41].

2. Experimental

2.1. Materials

Native corn starch (*Zea mays*), purchased from the Distribuidora Dos Hermanos, Mark Ying Yang (Mar del Plata, Argentina), and polystyrene (PS) pellets, supplied by Petrobras (trade name: INNOVA HF-555), were used to prepare the starch/PS blends. The catalyst (zinc octanoate - Zn(Oct)$_2$) (density = 1.13 g/mL, boiling point = 239.3 °C) was kindly provided by Ghion, Laboratorios Químicos, S.R.L. (Mar del Plata, Argentina) (approx. 10% w/w of Zn). Glycerol (density = 1.26 g/mL, boiling point = 290 °C) from Aurum (Mar del Plata, Argentina) was employed as the plasticizer for film formation.

2.2. Modification of starch

Native corn starch was modified by oxidation with hydrogen peroxide (H$_2$O$_2$). To do this, 1 Kg of starch (dry basis) was placed into a reactor previously charged with 4.2 L of distilled water. The pH was adjusted to 9 by slowly adding a sodium hydroxide (NaOH) solution (2 M) while mechanically stirring at 200 rpm for 15 min. Then, 126 mL of H$_2$O$_2$ (20% v/v) were also slowly added. The blend was reacted for the next 2 h at room temperature (25 °C) while agitating at 200 rpm, after which time the pH was lowered to 7 with a 2.5% HCl solution. The slurry was then washed three times by suspension in distilled water, centrifuged at 1500 rpm

for 15 min and dried in an oven at 45 °C for 24 h. Finally, the dried modified starch was milled and passed through a 60-mesh sieve.

2.3. Characterization of the starches

Total amylose content was determined by the thermogravimetric analysis (TGA) method described by Stawski [42]. The carboxyl and carbonyl content of the oxidized starch was determined according to Yi, Zhang, & Ju, [43]. The morphology of the starch granules was observed using optical microscopy [44,45]. The infrared (*IR*) spectra of the starches were recorded in a Nicolet 8700 Fourier transform infrared spectrometer, with the diamond crystal at an incident angle of 45°. Spectra were obtained by recording 40 scans performed with a resolution of 4 cm^{-1} between 600 and 4000 cm^{-1}. The heat flow curves of the starches were determined using a differential scanning calorimeter (Perkin Elmer, Pyris 1). A sample weight of approximately 10 mg was packed and sealed in a high pressure aluminum pan. The reference was an empty aluminum pan. Samples were heated to between 20 °C and 250 °C at a constant heating rate of 10 °C/min. The gelatinization temperature (T$_{gelatinization}$) was obtained from the middle temperature in the relaxation range of the heat flow curves and the gelatinization enthalpy (ΔH$_g$) was estimated as the area below the gelatinization peak. Two samples of each starch were tested. Thermogravimetric tests (*TGA*) were carried out with the aid of a TA Model TGA Q500. Samples were heated at a constant rate of 10 °C/min from room temperature to 500 °C, under nitrogen atmosphere. The characteristic decomposition temperature of each starch was then determined from the thermogravimetric (*DTG*) curves obtained.

2.4. Extrusion and film formation

Films were prepared from native and modified corn starch/PS blends at a 50:50 ratio (210 g of starch and 210 g of PS) plus 90 g of glycerol. To some of the samples 8 g of the catalyst were then also added. The blends were homogenized manually before being introduced into the extruder. The instrument used was a twin-screw extruder with six heating zones and two feed zones. The first feed zone is in the first heating step, and the second is in the third heating step. The extrusion profile chosen was 165/170/170/180/190/195 °C. Films were obtained by compressing at 180 °C for 15 min. at 100 bars, and then cooling to 30 °C. Four film systems were obtained as follows: native corn starch + polystyrene (TPS-NCS + PS), native corn starch + polystyrene + catalyst (TPS-NCS + PS + CAT), oxidized corn starch + polystyrene (TPS-OCS + PS) and oxidized corn starch + polystyrene + catalyst (TPS-OCS + PS + CAT). The resultant materials were conditioned with a saturated solution of NaBr (a$_w$ ~ 0.575 at 25 °C) for seven days prior to each test.

2.5. Characterization of the films

2.5.1. Determination of the average molecular weight (M$_w$) of the developed films using an Ostwald viscometer

An Ostwald viscometer (Cannon-Fenske 200 series, model 120,205, IVA, Argentina) at 25.0 ± 0.1 °C was used to estimate the molecular weight of the developed films. Average molecular weight was determined using the procedure described by Gutiérrez, & González [4,46], which is based on the capillary viscometry of polymers. The Mark-Houwink-Sakurada-Staudinger equation (Eq. (1)), empirically demonstrated by Kramer [47] and Huggins [48], was employed as a calculation tool as follows:

$$M_w = \left(\eta / K \right)^{1/a} \tag{1}$$

where:

M$_w$ = polymer molecular weight.
η = intrinsic viscosity.

K and ^{a} = constants reported for the solvent used (Dimethyl sulfoxide).

K = 0.0112 mL/g at 25 °C.

^{a} = 0.72 at 25 °C.

The molecular weight experiments were conducted in triplicate, and data were reported as mean values ± SD.

2.5.2. Moisture content (MC)

Square-shaped samples (4 cm^2) were weighed using an analytical balance (±0.0001 g; Ohaus, USA) in order to determine their initial mass (m_i). Samples were then dried in an oven at 105 ± 1 °C for 24 h (Memmert, Germany). Moisture content was determined as the percentage of water lost during drying:

$$MC (\%) = (m_i - m_d) \times m_i^{-1} \times 100 \tag{2}$$

where m_i and m_d are the initial and final (dry) masses of the films, respectively. Three samples of each film system were measured. Results were reported as % average moisture ± SD.

2.5.3. Attenuated total reflectance Fourier transform infrared spectroscopy (ATR/FTIR)

A Nicolet 8700 (Thermo Scientific Instrument Co., Madison, Wisconsin, USA) equipped with a diamond ATR probe at an incident angle of 45° was used to collect the infrared spectra of the film samples. Infrared spectra were recorded over the range 4000–600 cm^{-1} from 32 co-added scans at 4 cm^{-1} resolution. Each sample was scanned three times, observing good reproducibility.

2.5.4. Water solubility (WS)

Water solubility was determined according to the method described by Gutiérrez, Morales, Pérez, Tapia, & Famá, [49]. Solubility is defined as the content of dry matter solubilized after 24 h immersion in water. The initial dry matter content of each film system was determined by drying to a constant weight in an oven (Memmert, Germany) at 105 °C. Film pieces were cut (2 × 2 cm) and the initial weights registered (w_i). The films were then immersed in 50 mL of distilled water and stored for 24 h at 25 °C in a low temperature incubator (Heraeus, model BK 600, range: 3–40 °C, Hanau, Germany). After this, samples were filtered through previously desiccated and weighed filter paper, and the undissolved films obtained were dried to constant weight (w_f) in an oven at 105 °C for 24 h to determine the weight of dry matter that was not solubilized in water. The solubility of each film was then determined as follows:
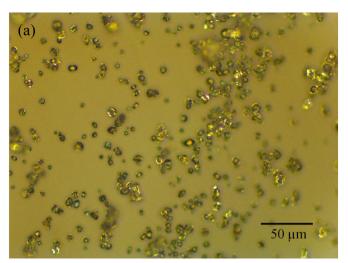
$$WS (\%) = \frac{(W_i - W_f)}{W_i} \times 100 \tag{3}$$

where w_i is the initial weight, and w_f the final weight of the sample. The average value from three measurements ± SD was reported.

2.5.5. Thermogravimetric analysis (TGA)

A thermal analyzer (TA Instruments) Model TGA Q500 (Hüllhorst, Germany) at a heating rate of 10 °C/min from room temperature to 500 °C under nitrogen atmosphere (gas flow 30 mL/min) was used to perform the thermogravimetric analysis. Film weights were in the range of 7–15 mg. The weight loss of materials was then recalculated on dry basis and the different degradation phases noted. Analyses were performed in triplicate to ensure repeatability.

2.5.6. Differential scanning calorimetry (DSC)

The melting temperatures (T_m) of the films were determined using a DSC Pyris 1 from Perkin Elmer (Massachusetts, USA). Temperature and heat flux were previously calibrated using indium and zinc. Samples of about 5 mg of each system were contained in hermetically sealed aluminum pans and heated from room temperature up to 200 °C at a scanning
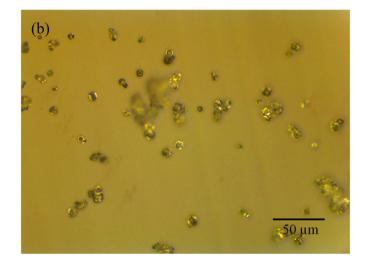

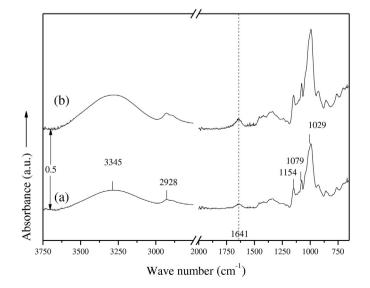**Fig. 1.** Optical micrographs at 20× of the granules of: (a) native corn starch and (b) oxidized corn starch.

rate of 10 °C/min, under nitrogen atmosphere. Changes of phase or state and the corresponding enthalpies were determined from the melting

Fig. 2. FTIR spectra of the starches used in all the absorption range: (a) native corn starch and (b) oxidized corn starch.
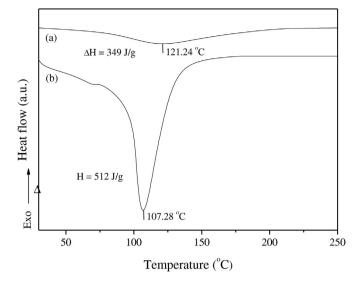
Fig. 3. DSC thermograms of the starches used: (a) native corn starch and (b) oxidized corn starch.

peaks of the DSC thermograms [50,51]. Three samples were analyzed for each film system.

2.5.7. X-ray diffraction (XRD)

A PAN analytical X'Pert PRO diffractometer (Netherlands) equipped with a monochromatic CuKa radiation source (λ = 1.5406 Å) operating at 40 kV and 40 mA at a scanning rate of 1° per min was used to obtain the X-ray diffractograms of the films. Samples were scanned in a 2θ range, varying from 3 to 33°. The thicknesses of the samples on the slides were ~680 μm. The crystalline fractions were estimated by drawing a smooth curve through the bases of the main peaks (main *d*-spacings) [52], and then using the following equation:

$$\text{Crystallinity} (\%) = \frac{\text{Area above the smooth curve}}{\text{Total area below the XRD spectrum}} \times 100 \quad (4)$$

2.5.8. Stability in acidic or alkaline solutions

The stability of the films in acidic and alkaline solutions was evaluated. Circular-shaped samples (diameter ~ 12 mm) were immersed in plastic petri dishes with 20 mL of standard HCl (pH 1 / 0.1 M) or NaOH (pH 13/0.1 M) solutions. The containers were then sealed and maintained at 25 °C for 30 days. Changes in the appearance of the samples were recorded with an 8.1 mega pixel Cyber-shot Sony camera, model DSC-H3. Tests were performed in triplicate for each system.

2.5.9. Scanning electron microscopy (SEM)

SEM micrographs of the cryo-fractured surfaces of samples were taken using a JEOL JSM-6460 LV instrument. For this, film pieces were mounted on bronze stubs and sputter-coated (Sputter coater SPI Module, Santa Clara, CA, USA) with a thin layer of gold for 35 s.

2.5.10. Uniaxial tensile tests

An INSTRON 4467 machine was used to measure the mechanical properties of the developed films following the ISO 527-2 norm [53]. Film strips (10 per formulation) were mounted in the tensile grips (A/TG model) and stretched at a rate of 0.01 mm/s until they broke. Tests were conducted in an ambient temperature of 25 °C, and relative humidity around 57%.

The force-distance curves obtained in the tests were transformed into stress-strain curves from which the following parameters were

calculated: Young's modulus (E), maximum stress (σ_m), strain at break (ε_b) and toughness (T).

2.5.11. Antimicrobial activity

Antimicrobial activity tests of the films and the catalyst were carried out using the agar diffusion method according to Ponce, Fritz, Del Valle, & Roura, [54]. Films were cut into circular-shaped discs (diameter 12 mm). They were then hydrated with 1 mL of sterile water and placed on Mueller Hinton agar (Merck, Darmstadt, Germany) plates previously seeded with 0.1 mL of inoculums containing approximately 10^5–10^6 CFU/mL of test bacteria. The zone of inhibition assay on solid media was used for determining the antimicrobial effects of the films against three typical pathogens: a Gram-negative bacteria, *Escherichia coli O157:H7* (32158, American Type Culture Collection) and two Gram-positive bacteria, *Listeria monocytogenes innocua* and *Staphylococcus aureus*, provided by CERELA (Centro de Referencia de Lactobacilos, Tucumán, Argentina). For this, the plates were incubated for 24 h at 37 °C, and then examined to study the inhibitory effect. The total area was used to evaluate the antimicrobial potential of films by exactly measuring the diameter of the inhibitory zones surrounding the wells as well as the contact area of these with the agar surface. The films were then classified using the diameters of the inhibition halos as: not sensitive for diameters <8 mm; sensitive for diameters of 9–14 mm; very sensitive for diameters of 15–19 mm and extremely sensitive for diameters larger than 20 mm [54]. Experiments were done in triplicate on two separate experimental runs.

2.6. Statistical analysis

OriginPro 8 (Version 8.5, Northampton, USA) was used to analyze the resulting data. Data were initially evaluated by an analysis of variance (ANOVA) test, and significant results were further analyzed using Duncan's multiple range tests ($p < 0.05$) to compare the mean values of the film properties studied.

3. Results and discussion

3.1. Characterization of the starches

The apparent amylose content of the native and modified starches was ~19% and ~17%, respectively. As is well known, the oxidation of starch produces new functional groups and breaks the cyclic structure of the basic units of the monosaccharide constituting the starch, i.e. glucose. The linear structure of the amylose is thus lost during the oxidation reaction leading to a reduction in the amylose content. However, in no
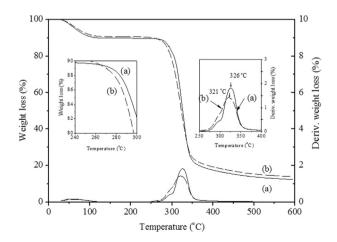

Fig. 4. TGA and DTGA curves of the starches used: (a) native corn starch and (b) oxidized corn starch.

case can this new structure, a product of the oxidation of starch, be considered as amylopectin, since amylopectin is a macromolecule and a structural isomer of amylose. The carboxyl and carbonyl contents in the oxidized starch were ~0.05% and ~0.21%, respectively. Similar results were reported by Wang & Wang [55] for oxidized corn starch which they obtained using different levels of sodium hypochlorite as a modifying agent.

The optical micrographs taken revealed that the starch granules of the native and oxidized corn were small to large in size and oval to polyhedral in shape (Fig. 1 a and b). In this study, however, no noticeable differences in their appearances were observed. This demonstrates that the hydrogen peroxide used to oxidize the starch did not cause any significant changes to the morphology of the starch granules. Similar results were reported by Sandhu et al. [56] for corn starch oxidized with different levels of sodium hypochlorite.

The FTIR spectra of the native and oxidized corn starches are shown in Fig. 2. Similar spectra have been reported in the literature for sagu starch [45]. The corn starch treated with hydrogen peroxide exhibited a peak at ~1641 cm^{-1}. This is associated with the symmetric stretching of carboxyl groups ($-$COO) thus confirming that the starch was oxidized.

The thermal transition curves of the native and oxidized corn starch observed using DSC are shown in Fig. 3. The oxidized corn starch systems showed lower $T_{gelatinization}$ compared to their native counterparts. The decrease in the $T_{gelatinization}$ of starch upon oxidation could be due to the weakening of the starch granules, resulting in the early rupture of the amylopectin double helices [57]. Wang & Wang [55] also found that the $T_{gelatinization}$ of oxidized normal and waxy corn starches were lower than their native counterparts. The ΔH_g was also higher in the oxidized corn starch than in the native starch. It is worth noting that higher values of $T_{gelatinization}$ and ΔH_g were registered in this study than elsewhere in the literature for corn starch oxidized with sodium hypochlorite [55,56,58].

The TGA results for the starches studied are shown in Fig. 4. These results are consistent with those obtained from the DSC analyses: the native corn starch showed higher $T_{gelatinization}$ and decomposition temperatures than the modified starch. Similar results have been reported for sagu starch [45], although in our case the degradation temperature values were approx. 10 °C above those measured by Gutiérrez, & Alvarez [45].

3.2. Characterization of the films

3.2.1. Average molecular weight (M_w) of the films developed

Table 1 shows the molecular weights of the different films studied. It is noteworthy that the molecular weights of the films developed from the oxidized starch/polystyrene blend (TPS-OCS) were significantly higher than those of the films prepared from the native starch/polystyrene blend (TPS-NCS). According to the literature, an increase in the molecular weight of polymers is related to a greater reactivity of the cross-linking reactions [40]. This suggests a crosslinking effect as well as an increase in the reactivity of the oxidized starch/polystyrene blends.

On the other hand, the increase in the molecular weights of the films could be due to the decrease in the total amylose content of the starches, brought on by the oxidation reaction: the oxidized corn starch films

(TPS-OCS + PS and TPS-OCS + PS + CAT) had the highest molecular weights. Results reported by Yoo, & Jane [59] for starches with low amylose contents are consistent with the results obtained here.

A statistically significant ($p \leq 0.05$) increase in the molecular weight of the films containing the catalyst may also be observed from Table 1, suggesting the occurrence of a cross-linking reaction between these starches and the polystyrene (PS). This fits well with that established in the literature [40]. Similar results were obtained by Gutiérrez, & González [4] for starch films slightly cross-linked by pulsed light. Finally, a most significant ($p \leq 0.05$) increase in molecular weight was obtained for the TPS-OCS + PS + CAT film, suggesting that the presence of the catalyst increased the reaction rate between the oxidized starch and the PS.

3.2.2. Moisture content (MC)

Table 1 shows the moisture contents of the different films studied. Films containing the catalyst (TPS-NCS + PS + CAT and TPS-OCS + PS + CAT) had a statistically significant ($p \leq 0.05$) lower moisture content compared to the films without the catalyst (TPS-NCS + PS and TPS-OCS + PS). This suggests that the catalyst caused a decrease in the polarity of the starch materials due to a cross-linking reaction between the starch and PS, thus limiting the water absorption capacity of the polar groups of these matrices [41,60]. Similar behavior was reported by Gutiérrez et al. [49,61] for films prepared from cassava and cush-cush yam starches chemically modified by cross-linking with sodium trimetaphosphate (STMP).

It is noteworthy that the cross-linking of native and oxidized starch chains occurs through the hydroxyl groups of this macromolecule, in which the hydroxyl groups act as nucleophiles in the addition reaction on the double bond of the styrene monomer. This lies at the terminal end of the polystyrene, thus demonstrating that the native and oxidized corn starch/PS blends are cross-linked by means of a catalyst [62].

The purpose of modifying the starch was to increase its reactivity in the presence of the catalyst in order to increase the degree of cross-linking between it (the now oxidized starch) and the PS, thus improving compatibility between these polymers. This was apparently achieved, since the molecular weights significantly increased when the catalyst was added. In addition, the oxidized corn starch/PS blend plus catalyst (TPS-OCS + PS + CAT) showed a greater reduction in the moisture content than the native corn starch/PS blend plus catalyst (TPS-NCS + PS + CAT). However, the carboxyl and carbonyl groups remained as polar sites (Lewis sites) within the structure, which allowed some water adsorption from the environment. This would explain the higher moisture content in the films prepared from the oxidized starch (TPS-OCS + PS and TPS-OCS + PS + CAT) compared to those prepared from native starch (TPS-NCS + PS and TPS-NCS + PS + CAT).

3.2.3. Attenuated total reflectance Fourier transform infrared spectroscopy (ATR/FTIR)
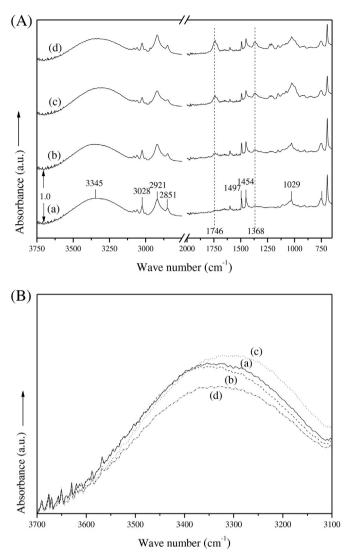
Fig. 5A shows the ATR/FTIR spectra of the different films studied over the whole absorption range. An important absorption peak at around 3345 cm^{-1} (stretching of the OH groups belonging to starch, glycerol and water) associated with a stretching vibration of the C-O groups was observed in all the systems studied [63,64]. According to González et al. [60] and Gutiérrez et al. [61] a material with OH groups that more

Table 1
Average molecular weight (M_w), moisture content (MC), water solubility (WS) and crystallinity of the different films.

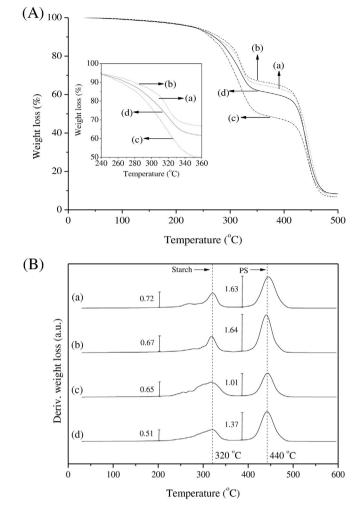| Parameter	TPS-NCS + PS	TPS-NCS + PS + CAT	TPS-OCS + PS	TPS-OCS + PS + CAT
M_w ($\times 10^8$ g/mol)	1.5 ± 0.2[a]	1.9 ± 0.1[b]	12.6 ± 0.3[c]	17.1 ± 0.2[d]
MC (%)	7.8 ± 0.5[b]	6.8 ± 0.4[a]	10.0 ± 0.8[d]	8.7 ± 0.1[c]
WS (%)	27 ± 2[b]	23 ± 1[a]	40 ± 5[d]	31 ± 2[c]
Crystallinity (%)	6.0 ± 0.2[d]	5.5 ± 0.2[c]	3.1 ± 0.1[b]	2.0 ± 0.1[a]

Equal letters in the same row indicate no statistically significant differences ($p \leq 0.05$).
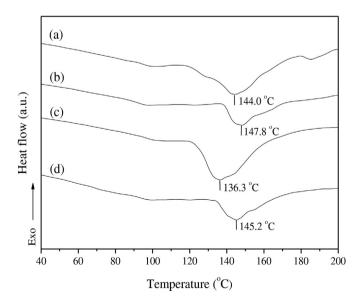
Fig. 5. Panel A- FTIR spectra of the different films studied in all the absorption range: (a) native corn starch + polystyrene (TPS-NCS + PS), (b) native corn starch + polystyrene + catalyst (TPS-NCS + PS + CAT), (c) oxidized corn starch + polystyrene (TPS-OCS + PS) and (d) oxidized corn starch + polystyrene + catalyst (TPS-OCS + PS + CAT). Panel B - FTIR spectra in the range of absorption corresponding to C—O group (OH stretching) of the different films studied: (a) native corn starch + polystyrene (TPS-NCS + PS), (b) native corn starch + polystyrene + catalyst (TPS-NCS + PS + CAT), (c) oxidized corn starch + polystyrene (TPS-OCS + PS) and (d) oxidized corn starch + polystyrene + catalyst (TPS-OCS + PS + CAT).

Fig. 6. (A) TGA and (B) DTGA curves of the different films studied: (a) native corn starch + polystyrene (TPS-NCS + PS), (b) native corn starch + polystyrene + catalyst (TPS-NCS + PS + CAT), (c) oxidized corn starch + polystyrene (TPS-OCS + PS) and (d) oxidized corn starch + polystyrene + catalyst (TPS-OCS + PS + CAT).

easily vibrate and/or form more hydrogen bond tends to present a wider and less intense band. This fits well with the results obtained, since, as can be clearly seen in the region between 3700 and 3100 cm^{-1} (Fig. 5B), the incorporation of the catalyst decreased the absorbance of this band. In addition, the lower intensity of the band associated with the OH groups could also be related to the lower moisture content and loss of the starch hydroxyl groups after the cross-linking of the polymeric chains. Similar results were recently reported by González et al. [60] for films prepared from cassava starch cross-linked with citric acid.
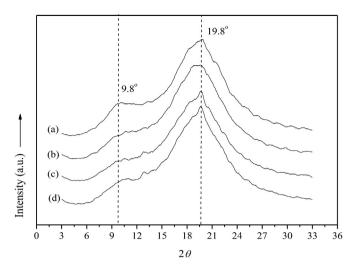
The peaks at 2851 and 2921 cm^{-1} are associated with C—H stretch vibrations [65] and are characteristic of polymeric matrix materials. Other bands appearing between 1368 cm^{-1} and 1497 cm^{-1} are assigned to C—O angular deformations [66]. Specifically, the band detected at ~1368 cm^{-1} for the oxidized corn starch-based films (TPS-OCS + PS and TPS-OCS + PS + CAT) is associated with the symmetric stretching of carboxyl groups (-COO) [67]. This band was not evident

Fig. 7. Heating thermograms of the films based on: (a) native corn starch + polystyrene (TPS-NCS + PS), (b) native corn starch + polystyrene + catalyst (TPS-NCS + PS + CAT), (c) oxidized corn starch + polystyrene (TPS-OCS + PS) and (d) oxidized corn starch + polystyrene + catalyst (TPS-OCS + PS + CAT).

Fig. 8. X-ray diffraction pattern of the different films studied: (a) native corn starch + polystyrene (TPS-NCS + PS), (b) native corn starch + polystyrene + catalyst (TPS-NCS + PS + CAT), (c) oxidized corn starch + polystyrene (TPS-OCS + PS) and (d) oxidized corn starch + polystyrene + catalyst (TPS-OCS + PS + CAT).

in the systems prepared from blends with native corn starch (TPS-NCS + PS and TPS-NCS + PS + CAT).

The band located at 1746 cm^{-1} in films containing the catalyst could be assigned to C=O groups from ester groups formed between the starch and PS, confirming the cross-linking effect proposed (Fig. 5A). It is interesting that the increase in peak intensity was more marked in the TPS-OCS + PS + CAT film compared to the TPS-NCS + PS + CAT film, suggesting a higher degree of cross-linking between the oxidized starch and PS in the presence of the catalyst. Similar results were reported by González et al. [60] for films derived from cassava starch cross-linked with citric acid. It is worth noting that this band was also

observed in the TPS-OCS + PS film but not in the TPS-NCS + PS film. This is due to the carboxyl and carbonyl groups contained within the oxidized starch.

3.2.4. Water solubility (WS)

Table 1 shows the water solubility values at 25 °C for the different systems studied. As can be observed the native starch films were significantly less water soluble ($p \leq 0.05$) than the oxidized starch films, suggesting an increase in the hydrophilicity of these systems. This is because the carboxyl and carbonyl groups in the oxidized starch act as Lewis sites (polar sites) thus increasing their water solubility. These results agree with those given by Gutiérrez et al. [1] for native and phosphated *Zea mays* starch-based films.
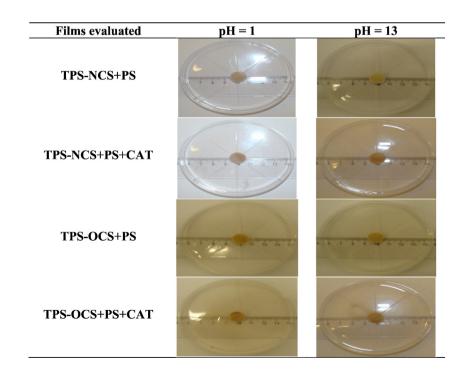
On the other hand, it can be seen that the catalyst-containing films (TPS-NCS + PS + CAT and TPS-OCS + PS + CAT) were significantly less water soluble ($p \leq 0.05$) than the films without the catalyst (TPS-NCS + PS and TPS-OCS + PS). The water solubility of starch films provides an indication of their integrity in an aqueous medium, such that higher solubility values indicate a lower water resistance [68]. The addition of the catalyst thus improved the water resistance of the film systems, which can also be related to the cross-linking reaction between the starch and PS. These results agree with the moisture content analyses.

A more significant reduction in the hydrophilicity of the TPS-OCS + PS + CAT film may be due not only to the crosslinking effect of the catalyst, but also to the hydrogen bond interactions established between the oxidized starch-plasticizer and the oxidized starch-oxidized starch. This would compensate for an increase in the polar sites of this material.

3.2.5. Thermogravimetric analysis (TGA)

Fig. 6 shows the TGA and DTGA (derivative TGA) curves for all the systems under study. This assay was conducted in order to analyze the thermal stability and compatibility of the four types of film evaluated.

The systems developed presented three stages that have been widely reported in the literature [49,61]: water evaporation, decomposition

Fig. 9. Digital photographs of the thermoplastic starch films immersed in acid and alkaline medium after 30 days: (a) native corn starch + polystyrene (TPS-NCS + PS), (b) native corn starch + polystyrene + catalyst (TPS-NCS + PS + CAT), (c) oxidized corn starch + polystyrene (TPS-OCS + PS) and (d) oxidized corn starch + polystyrene + catalyst (TPS-OCS + PS + CAT).

Fig. 10. SEM micrographs of the cryogenic fracture surface of the films based on: (a) native corn starch + polystyrene (TPS-NCS + PS), (b) native corn starch + polystyrene + catalyst (TPS-NCS + PS + CAT), (c) oxidized corn starch + polystyrene (TPS-OCS + PS) and (d) oxidized corn starch + polystyrene + catalyst (TPS-OCS + PS + CAT). At 1 kX of magnification.

of the glycerol-rich phase which also contains starch and lastly the PS decomposition stage. The first stage was not observed, since the curves were normalized on dry basis to avoid distortions as a result of the different initial moisture contents of the films tested [49,61].
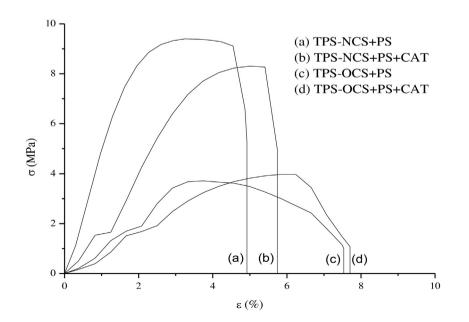
The first fact worth noting from the TGA curves is the double weight loss shown by all the prepared films (Fig. 6A) demonstrating that phase separation occurred between the polymers. This was confirmed by the presence of two decomposition peaks in the DTGA curves (Fig. 6B). The first peak corresponds to the decomposition temperature of the glycerol-rich phase containing starch (around 320 °C), and the second to the decomposition temperature of PS (around 440 °C) [7]. Thus, the incorporation of the catalyst did not prevent phase separation in the systems evaluated, although the compatibility of the polymers was improved. This was more evident in the blends made from oxidized starch (TPS-OCS + PS + CAT), demonstrating that the performance of the catalyst in generating a higher cross-linking rate was greater in this system

compared to the native starch blend (TPS-NCS + PS + CAT). In other words, the oxidized starch and PS became more reactive in the presence of the catalyst. Unfortunately, however, the number of Lewis sites within the oxidized starch increased, leading to a greater degree of phase separation in these systems (TPS-OCS + PS and TPS-OCS + PS + CAT) compared to the native starch/PS blends (TPS-NCS + PS and TPS-NCS + PS + CAT). This can also be observed from the TGA (Fig. 6A) where the curves corresponding to the oxidized starch systems are shifted to a lower temperature, indicating that the intra-molecular interactions between the components of these blends are weaker. This fits well with the results of the moisture content of these systems, since weak intra-molecular interactions would allow the glycerol to interact with other surrounding polar compounds, resulting in greater moisture absorption from the environment.

Moreover, Fig. 6B shows a more significant increase in weight loss in the TPS-OCS + PS + CAT film than in the TPS-NCS + PS + CAT film compared to their respective analogous films, within the range of the PS decomposition temperature. This is consistent with the fact that this system (TPS-OCS + PS + CAT) showed the highest molecular weight. This provides further evidence for the increase in the degree of cross-linking between the oxidized starch and PS in the presence of the catalyst.

3.2.6. Differential scanning calorimetry (DSC)

Fig. 7 shows the DSC curves for the developed films. According to Raquez et al. [69], these types of systems undergo changes in heat flow in the 140–160 °C range, which can be related to the melting temperature (T_m) of the crystalline section. As a general rule, any structural feature that reduces the mobility of the polymer chains or the free volume will increase the T_m [61,70–75]. The increase in T_m in systems containing the catalyst can thus be attributed to an increase in the cohesive forces of attraction between the polymer chains, as a result of cross-linking between the starch chains and PS. This is consistent with the results discussed above. Schlemmer et al. [76] obtained similar results for TPS/PS blends prepared with different plasticizers.

A more significant increase in T_m was obtained for the TPS-OCS + PS + CAT film than for the TPS-NCS + PS + CAT film compared with their respective analogous films, thus agreeing with the results previously discussed. As mentioned above, a higher degree of cross-linking was obtained in the TPS-OCS + PS + CAT film.

Fig. 11. Stress (σ)-strain (ε) curves of the films based on: (a) native corn starch + polystyrene (TPS-NCS + PS), (b) native corn starch + polystyrene + catalyst (TPS-NCS + PS + CAT), (c) oxidized corn starch + polystyrene (TPS-OCS + PS) and (d) oxidized corn starch + polystyrene + catalyst (TPS-OCS + PS + CAT).

3.2.7. X-ray diffraction (XRD)

Fig. 8 shows the X-ray diffraction patterns of the films studied. As can be seen, all the systems were composed principally of an amorphous phase with only a small crystalline fraction, thus agreeing with that previously reported for starch based films [49]. In general, the starch/PS films showed curves with diffraction peaks at $2\theta = 9.8$ and 19.8, corresponding to the d-spacings $\cong 9.0$ Å and 4.5 Å, respectively. All films showed A-type crystalline structures corresponding to peaks at $2\theta = 9.8$. In addition, peaks localized at $2\theta = 19.8$, related to the type-V structure, were observed. When glycerol is present the double helix conformations are disrupted by the formation of stable single chain V-conformation helices resulting in the glycerol-amylose complex [77–79].

According to Osella et al. [80], the development of A or B -type X-ray diffraction patterns in starch films depends partly on their water content. A decrease in moisture is highly correlated with an increase in the crystal phase of a semi-crystalline material [81,82]. Thus, the slightly higher crystallinity of the native corn starch films (TPS-NCS + PS and TPS-NCS + PS + CAT) compared to the oxidized starch films (Table 1) agrees with the lower humidity values obtained for these materials.

As mentioned above, native starch based films were more crystalline than those prepared from the oxidized starch (Table 1). According to Tapia et al. [83] and Pérez et al. [84], the crystallinity of starch films is mainly associated with the amylose content since this is almost linear, unlike amylopectin which is highly branched. This agrees with the other results reported in this paper.

Moreover, within each type of starch film (native or oxidized), lower crystallinity values were obtained for the catalyst-containing samples (Table 1). A similar phenomenon was observed by González et al. [60] for films prepared from cassava starch cross-linked with citric acid. Thus, the addition of the catalyst results in more amorphous materials Finally, crosslinking between the starch and PS was confirmed.

3.2.8. Stability in acidic or alkaline solutions

One of the main aims of this study was to evaluate whether films derived from corn starch/PS blends could be used in the food packaging industry. Many food products are either slightly acidic or slightly alkaline. It is thus important to determine whether the stability of the films used to wrap or coat foods is affected by pH.

In order to study the stability of the starch/PS-based films, samples of all systems were immersed in either an acid or an alkali medium. After 30 days in the acidic (HCl) or alkaline (NaOH) solutions, no visual change was observed in any of the film systems studied (Fig. 9). This suggests that they are stable in both acid and alkaline mediums and could thus be used for packaging slightly acidic and alkaline food products.

It is important to note that all the films studied showed greater stability in the alkaline medium than other oxidized starch-based films reported in the literature [61,82].

3.2.9. Scanning electron microscopy (SEM)

Fig. 10 shows the SEM images of the cryo-fractured surfaces of the different films. Heterogeneity was observed in all cases, thus demonstrating the lack of miscibility between the polymers studied (starch

and PS). This is consistent with the results of the TGA. Similar structures were reported by Gutiérrez, & Alvarez [45].

In addition, the blends showed poor interfacial adhesion due to the differences in their polarities [85,86]. Specifically, the films prepared from native corn starch (TPS-NCS + PS and TPS-NCS + PS + CAT, Fig. 10 a and b, respectively) had a "rougher" surface than those prepared from oxidized corn starch (TPS-OCS + PS and TPS-OCS + PS + CAT, Fig. 10 c and d, respectively). This was probably caused by the presence of native starch granules which were not fully plasticized during the extrusion process, since as discussed above the native corn starch showed the highest $T_{gelatinization}$.

According to Gutiérrez & González [4,46] and Gutiérrez et al. [61], a more compact structure leads to lower water adsorption as it makes interactions between the starch-glycerol and water less likely, leading to a decrease in the polar glycerol-starch character of the films [87]. This does not fit with the other results obtained in this study. However, in the next section we demonstrate that the morphology of the films did correlate with the mechanical behaviors observed. With this in mind, some authors [88] have associated smooth zone formations with improved mechanical properties.

3.2.10. Uniaxial tensile tests

The stress-strain curves of each developed film are shown in Fig. 11. A small linear elastic zone followed by a non-linear zone was observed until break point in the films without the catalyst (TPS-NCS + PS and TPS-OCS + PS). However, in the catalyst-containing films (TPS-NCS + PS + CAT and TPS-OCS + PS + CAT) a creep zone was observed. This behavior indicates a change in mechanical behavior from an elastic zone to a plastic zone, and was irreversible from 0.8% elongation in the TPS-NCS + PS + CAT film and 1.6% elongation in the TPS-OCS + PS + CAT film. In other words, theoretically, after elastic deformation these materials undergo a volume change. In addition, the TPS-NCS + PS + CAT film had a smaller creep zone than the TPS-OCS + PS + CAT film. It is well known that after the creep zone Hooke's Law for elastic, linear and isotropic materials is not met. This means that normal deformation does not occur anywhere in the solid, or along any of the direction of the normal stresses in the orthogonal directions, i.e. the principal directions of the stress matrix do not coincide with the principal direction of the matrix of deformation.

In addition, the positive slope of the curve in the plastic deformation range for the films containing the catalyst implies that hardening occurs until the sample finally breaks. This can be related to the polymer chains aligned parallel to the load [7] and fits well with the cross-linking mechanism proposed for these systems (TPS-NCS + PS + CAT and TPS-OCS + PS + CAT).

It is worth noting that for different food packaging applications, the duration of stress, temperature and applied load should also be considered, since the mechanical behavior observed for the catalyst-containing films (TPS-NCS + PS + CAT and TPS-OCS + PS + CAT) would signify the failure of these materials in a kinematic system.

Strain at break and maximum stress were not statistically different ($p \geq 0.05$) between the films that incorporated the catalyst (TPS-NCS + PS + CAT and TPS-OCS + PS + CAT) and the films that did not (Table 2). Similar strain at break and maximum stress values for films

Table 2
Parameters of the uniaxial tensile strength tests: Young's modulus (E), maximum stress (σ_m), strain at break (ε_b) and toughness (T).

Material	E (MPa)	σ_m (MPa)	ε_b (%)	T ($\times 10^3$) ($\mathbf{J/m^3}$)
TPS-NCS + PS	3.2 ± 0.6[d]	9.5 ± 0.4[b]	6 ± 1[a]	41.80 ± 0.01[d]
TPS-NCS + PS + CAT	1.9 ± 0.1[c]	8.9 ± 0.6[b]	6.3 ± 0.5[a]	36.13 ± 0.01[c]
TPS-OCS + PS	1.1 ± 0.1[b]	3.7 ± 0.3[a]	8.4 ± 0.6[b]	19.70 ± 0.01[b]
TPS-OCS + PS + CAT	0.94 ± 0.04[a]	3.8 ± 0.3[a]	7.7 ± 0.5[b]	18.03 ± 0.01[a]

Equal letters in the same column indicate no statistically significant difference ($p \leq 0.05$).
Thermoplastic starch (TPS) films: native corn starch + polystyrene (TPS-NCS + PS), native corn starch + polystyrene + catalyst (TPS-NCS + PS + CAT), oxidized corn starch + polystyrene (TPS-OCS + PS) and oxidized corn starch + polystyrene + catalyst (TPS-OCS + PS + CAT).
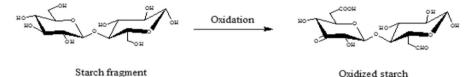
obtained from 50/50 cassava starch/PS blends prepared by melt blending were reported by Berruezo et al. [7]. However, the films derived from oxidized corn starch had a ductile behavior unlike the native corn starch films, which were far more fragile. This is in line with the DSC results: higher values of T_m were found for the films made from native corn starch/PS blends (TPS-NCS + PS and TPS-NCS + PS + CAT), indicating a lower mobility of the polymer chains. In other words, the macromolecules of these materials are more rigid making them more fragile. Similar behavior was observed by Gutiérrez et al. [89] for chemically modified starch-based films cross-linked with sodium

trimetaphosphate, and by García-Tejeda et al. [87] for films made from native and oxidized banana starch.

Other authors have also related the elasticity of starch films to their structure, indicating that higher elasticity values are associated with materials with a more compact structure [45,89]. This is consistent with our results, since the films prepared from the oxidized corn starch/PS blends showed a more compact morphology (Fig. 10 c and d) and were also more elastic.

The results of the mechanical tests are given in Table 2. It can be seen that the Young's modulus of samples ranged from 0.94 to 3.2 MPa, being
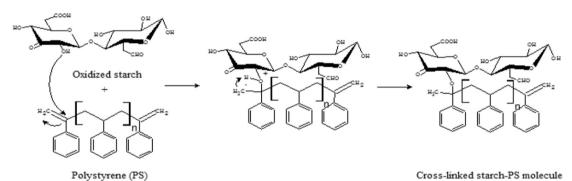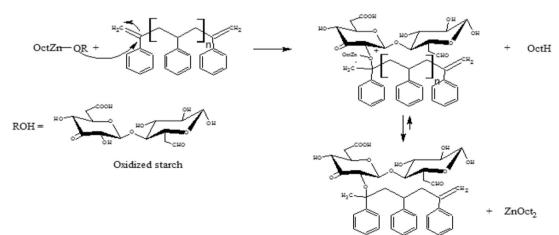

Fig. 12. Reaction mechanism proposed between starch and polystyrene with and without the presence of zinc octanoate.

lowest value obtained for the blend with the oxidized starch and the catalyst. Nevertheless, all the films obtained were at least four times more rigid than films derived from sagu starch/poly(ε-caprolactone) (PCL) blends obtained by melt mixing followed by compression molding [45].

Finally, the highest toughness value was obtained for the TPS-NCS + PS film. According to Gutiérrez, & Alvarez [45] and Gutiérrez et al. [90], this could be very useful, since these films could absorb more energy thus minimizing damage caused by knocks to foods during transport and storage. All the toughness values reported here are at least ten times higher than those for films made from sagu starch/PCL blends [45].

3.2.11. Antimicrobial activity

The antimicrobial capacity of the four film systems was evaluated in order to establish whether they had potential as active packaging materials. However, none of films analyzed showed antimicrobial activity against the three test pathogenic microorganisms (*Escherichia coli O157:H7*, *Listeria monocytogenes innocua* and *Staphylococcus aureus*). In contrast, the catalyst ($Zn(Oct)_2$) exhibited an excellent antimicrobial effect: 35 mm, 35 mm and 25 mm against *E. coli O157:H7*, *L. monocytogenes innocua* and *S. aureus*, respectively. These, apparently conflicting, results may be explained by the fact that only a very low amount of the catalyst (approx. 1.90%) was present in each blend, and thus its antimicrobial effect was not manifested. The results are, however, promising, since they suggest that this catalyst could have a secondary function in REx processes. Finally, based on the results obtained, the following reaction mechanism can be proposed (Fig. 12).

4. Conclusions

Films made from native and oxidized starch/PS blends were obtained under conditions of reactive extrusion (REx). The catalyst used, ($Zn(Oct)_2$), showed a strong antimicrobial effect against both Gram-positive and Gram-negative pathogenic microorganisms (*E. coli O157:H7*, *L. monocytogenes innocua* and *S. aureus*). However, the films developed from the starch/PS blends containing the catalyst showed no antimicrobial activity. Nevertheless, the catalyst promoted the cross-linking of the starch/PS blends, especially when coupled with the oxidized starch. Finally, phase separation was observed in all the systems studied, although the mass fraction of each phase was different with and without the catalyst. Thus, although the catalyst produced the formation of the most thermo-resistant fractions, particularly in the blends incorporating oxidized starch, phase separation was more marked in these blends than in the film systems derived from native starch/PS.

Conflicts of interest

The authors declares no conflict of interest.

Acknowledgements

References

[1] T.J. Gutiérrez, N.J. Morales, M.S. Tapia, E. Pérez, L. Famá, Corn starch 80:20 "waxy": regular, "native" and phosphated, as bio-matrixes for edible films, Proc. Mater. Sci. 8 (2015) 304–310.

[2] U. Arena, M.L. Mastellone, F. Perugini, Life cycle assessment of a plastic packaging recycling system, Int. J. Life Cycle Assess. 8 (2003) 92–98.

[3] M.C. Li, J.K. Lee, U.R. Cho, Synthesis, characterization, and enzymatic degradation of starch-grafted poly (methyl methacrylate) copolymer films, J. Appl. Polym. Sci. 125 (2012) 405–414.

[4] T.J. Gutiérrez, G. González, Effects of exposure to pulsed light on surface and structural properties of edible films made from cassava and taro starch, Food Bioprocess Technol. 9 (2016) 1812–1824.

[5] M.C. Li, X. Ge, U.R. Cho, Emulsion grafting vinyl monomers onto starch for reinforcement of styrene-butadiene rubber, Macromol. Res. 21 (2013) 519–528.

[6] M.C. Li, U.R. Cho, Effectiveness of coupling agents in the poly (methyl methacrylate)-modified starch/styrene-butadiene rubber interfaces, Mater. Lett. 92 (2013) 132–135.

[7] M. Berruezo, L.N. Ludueña, E. Rodriguez, V.A. Alvarez, Preparation and characterization of polystyrene/starch blends for packaging applications, J. Plast. Film Sheet. 30 (2014) 141–161.

[8] T.J. Gutiérrez, M.P. Guarás, V.A. Alvarez, Reactive extrusion for the production of starch-based biopackaging, in: M. Masuelli (Ed.), Biopackaging, CRC Press, ISBN: 9781498749688, 2017 (in press).

[9] P. Dubois, R. Jerome, P. Teyssie, Macromolecular engineering of polylactones and polylactides, Polym. Bull. 22 (1989) 475–482.

[10] C. Jacobs, P. Dubois, R. Jérôme, P. Teyssié, Macromolecular engineering of polylactones and polylactides. 5. Synthesis and characterization of diblock copolymers based on poly-ε-caprolactone and poly (L, L or D, L) lactide by aluminum alkoxides, Macromolecules 24 (1991) 3027–3034.

[11] I. Barakat, P. Dubois, R. Jerome, P. Teyssié, Macromolecular engineering of polylactones and polylactides. X. Selective end-functionalization of poly (D, L)-lactide, J. Polym. Sci., Part A: Polym. Chem. 31 (1993) 505–514.

[12] Y.J. Du, P.J. Lemstra, A.J. Nijenhuis, H.A. Van Aert, C. Bastiaansen, ABA type copolymers of lactide with poly (ethylene glycol). Kinetic, mechanistic, and model studies, Macromolecules 28 (1995) 2124–2132.

[13] H.R. Kricheldorf, I. Kreiser-Saunders, C. Boettcher, Polylactones: 31. Sn (II) octoate-initiated polymerization of ʟ-lactide: a mechanistic study, Polymer 36 (1995) 1253–1259.

[14] N. Gaylord, Maleic Anhydride Grafting, CRC press Inc, New York, 1996.

[15] D. Carlson, L. Nie, R. Narayan, P. Dubois, Maleation of polylactide (PLA) by reactive extrusion, J. Appl. Polym. Sci. 72 (1999) 477–485.

[16] R. Mani, M. Battacharya, J. Tang, Functionalization of polyesters with maleic anhydride by reactive extrusion, J. Polym. Sci. A Polym. Chem. 37 (1999) 1693–1702.

[17] D. Mecerreyes, R. Jérôme, From living to controlled aluminium alkoxide mediated ring-opening polymerization of (di) lactones, a powerful tool for the macromolecular engineering of aliphatic polyesters, Macromol. Chem. Phys. 200 (1999) 2581–2590.

[18] W. Tang, N.S. Murthy, F. Mares, M.E. Mcdonnell, S.A. Curran, Poly (ethylene terephthalate)–poly (caprolactone) block copolymer. I. Synthesis, reactive extrusion, and fiber morphology, J. Appl. Polym. Sci. 74 (1999) 1858–1867.

[19] R.A. de Graaf, L.P.B.M. Janssen, The production of a new partially biodegradable starch plastic by reactive extrusion, Polym. Eng. Sci. 40 (2000) 2086–2094.

[20] S. Penczek, A. Duda, A. Kowalski, J. Libiszowski, K. Majerska, T. Biela, On the mechanism of polymerization of cyclic esters induced by tin (II) octoate, Macromol. Symp. 157 (2000) 61–70.

[21] R.R.N. Sailaja, M. Chanda, Use of maleic anhydride-grafted polyethylene as compatibilizer for polyethylene-starch blends: effects on mechanical properties, J. Polym. Mater. 17 (2000) 165–176.

[22] M.R. Lutfor, M.Z.A. Rahman, S. Sidik, A. Mansor, J. Haron, W. Yunus, Kinetics of graft copolymerization of acrylonitrile onto sago starch using free radicals initiated by ceric ammonium nitrate, Des. Monomers Polym. 4 (2001) 253–260.

[23] B.J. Kim, J.L. White, Bulk polymerization of ε-caprolactone in an internal mixer and in a twin screw extruder, Int. Polym. Process. 17 (2002) 33–43.

[24] B.J. Kim, J.L. White, Continuous polymerization of lactam–lactone block copolymers in a twin-screw extruder, J. Appl. Polym. Sci. 88 (2003) 1429–1437.

[25] B.J. Kim, J.L. White, Engineering analysis of the reactive extrusion of ε-caprolactone: the influence of processing on molecular degradation during reactive extrusion, J. Appl. Polym. Sci. 94 (2004) 1007–1017.

[26] I. Kim, J.L. White, Reactive copolymerization of various monomers based on lactams and lactones in a twin-screw extruder, J. Appl. Polym. Sci. 96 (2005) 1875–1887.

[27] S. Wang, J. Yu, J. Yu, Compatible thermoplastic starch/polyethylene blends by one-step reactive extrusion, Polym. Int. 54 (2005) 279–285.

[28] L. Zhu, K.A. Narh, K.S. Hyun, Investigation of mixing mechanisms and energy balance in reactive extrusion using three-dimensional numerical simulation method, Int. J. Heat Mass Transf. 48 (2005) 3411–3422.

[29] J.M. Raquez, P. Degée, Y. Nabar, R. Narayan, P. Dubois, Biodegradable materials by reactive extrusion: from catalyzed polymerization to functionalization and blend compatibilization, Chimie 9 (2006) 1370–1379.

[30] N. Wang, J. Yu, X. Ma, Preparation and characterization of thermoplastic starch/PLA blends by one-step reactive extrusion, Polym. Int. 56 (2007) 1440–1447.

[31] K. Frost, J. Barthes, D. Kaminski, E. Lascaris, J. Niere, R. Shanks, Thermoplastic starch-silica-polyvinyl alcohol composites by reactive extrusion, Carbohydr. Polym. 84 (2011) 343–350.

[32] D. Song, Y.S. Thio, Y. Deng, Starch nanoparticle formation via reactive extrusión and related mechanism study, Carbohydr. Polym. 85 (2011) 208–214.

[33] P.J.P. Espitia, N.D.F.F. Soares, J.S. dos Reis Coimbra, N.J. de Andrade, R.S. Cruz, E.A.A. Medeiros, Zinc oxide nanoparticles: synthesis, antimicrobial activity and food packaging applications, Food Bioprocess Technol. 5 (2012) 1447–1464.

[34] R. Sothornvit, C.W. Olsen, T.H. McHugh, J.M. Krochta, Tensile properties of compression-molded whey protein sheets: determination of molding condition and glycerol-content effects and comparison with solution-cast films, J. Food Eng. 78 (2007) 855–860.

[35] M. Thunwall, V. Kuthanova, A. Boldizar, M. Rigdahl, Film blowing of thermoplastic starch, Carbohydr. Polym. 71 (2008) 583–590.

[36] M. Thunwall, A. Boldizar, M. Rigdahl, Compression molding and tensile properties of thermoplastic potato starch materials, Biomacromolecules 7 (2006) 981–986.

[37] S.K. Flores, D. Costa, F. Yamashita, L.N. Gerschenson, M.V. Grossmann, Mixture design for evaluation of potassium sorbate and xanthan gum effect on properties of tapioca starch films obtained by extrusion, Mater. Sci. Eng. C 30 (2010) 196–202.

[38] F.M. Pelissari, F. Yamashita, M.A. Garcia, M.N. Martino, N.E. Zaritzky, M.V.E. Grossmann, Constrained mixture design applied to the development of cassava starch–chitosan blown films, J. Food Eng. 108 (2012) 262–267.

[39] I. Šimkovic, Unexplored possibilities of all-polysaccharide composites, Carbohydr. Polym. 95 (2013) 697–715.

[40] M.W. Rutenberg, D. Solarek, E.F. Pachall, Starch derivates: properties and uses, in: R.L. Whistler, J.N. Bemiller (Eds.), Starch: Chemistry and Technology, second ed.Academic Press Inc, Orlando, FL, USA 1984, pp. 312–388.

[41] E. Olsson, M.S. Hedenqvist, C. Johansson, L. Järnström, Influence of citric acid and curing on moisture sorption, diffusion and permeability of starch films, Carbohydr. Polym. 94 (2013) 765–772.

[42] D. Stawski, New determination method of amylose content in potato starch, Food Chem. 110 (2008) 777–781.

[43] X. Yi, S. Zhang, B. Ju, Preparation of water-soluble oxidized starch with high carbonyl content by sodium hypochlorite, Starch-Stärke 66 (2014) 115–123.

[44] T.J. Gutiérrez, E. Pérez, R. Guzmán, M.S. Tapia, L. Famá, Physicochemical and functional properties of native and modified by crosslinking, dark-cush-cush yam (*Dioscorea trifida*) and cassava (*Manihot esculenta*) starch, J. Polym. Biopolym. Phys. Chem. 2 (2014) 1–5.

[45] T.J. Gutiérrez, V.A. Alvarez, Films made by blending poly (ε-caprolactone) with starch and flour from sagu rhizome grown at the venezuelan amazons, J. Polym. Environ. (2016)http://dx.doi.org/10.1007/s10924-016-0861-9 (In press).

[46] T.J. Gutiérrez, G. González, Effect of cross-linking with *Aloe vera* gel on surface and physicochemical properties of edible films made from plantain flour, Food Biotechnol. (2016)http://dx.doi.org/10.1007/s11483-016-9458-z (In press).

[47] E.O. Kramer, Molecular weight of celluloses and cellulose derivates, J. Ind. Eng. Chem. 30 (1938) 1200–1203.

[48] M.L. Huggins, The viscosity of dilute solutions of long-chain molecules. IV. Dependence on concentration, J. Am. Chem. Soc. 64 (1942) 2716–2718.

[49] T.J. Gutiérrez, N.J. Morales, E. Pérez, M.S. Tapia, L. Famá, Physico-chemical properties of edible films derived from native and phosphated cush-cush yam and cassava starches, Food Packag. Shelf Life 3 (2015) 1–8.

[50] R.P. Chartoff, E.A. Turi, Thermal Characterization of Polymeric Materials, Vol. 1, Academic Press, USA, 1981 C 3.

[51] C.G. Biliaredis, A. Lazaridou, I. Arvanitoyannis, Glass transition and physical properties of polyol-plasticised pullulan-starch blends at low moisture, Carbohydr. Polym. 40 (1999) 29–47.

[52] P.H. Hermans, A. Weidinger, On the determination of the crystalline fraction of polyethylenes from X-ray diffraction, Macromol. Chem. Phys. 44 (1961) 24–36.

[53] ISO 527-2, Plastics–Determination of Tension Properties–Part, 1996 2.

[54] A.G. Ponce, R. Fritz, C. Del Valle, S.I. Roura, Antimicrobial activity of essential oils on the native microflora of organic Swiss chard, LWT-Food Sci. Technol. 36 (2003) 679–684.

[55] Y.J. Wang, L. Wang, Physicochemical properties of common and waxy corn starches oxidized by different levels of sodium hypochlorite, Carbohydr. Polym. 52 (2003) 207–217.

[56] K.S. Sandhu, M. Kaur, N. Singh, S.T.A. Lim, A comparison of native and oxidized normal and waxy corn starches: physicochemical, thermal, morphological and pasting properties, LWT Food Sci. Technol. 41 (2008) 1000–1010.

[57] K.O. Adebowale, O.S. Lawal, Functional properties and retrogradation behaviour of native and chemically modified starch of mucuna bean (*Mucuna pruriens*), J. Sci. Food Agric. 83 (2003) 1541–1546.

[58] D. Kuakpetoon, Y.J. Wang, Locations of hypochlorite oxidation in corn starches varying in amylose content, Carbohydr. Res. 343 (2008) 90–100.

[59] S.H. Yoo, J.L. Jane, Molecular weights and gyration radii of amylopectins determined by high-performance size-exclusion chromatography equipped with multi-angle laser-light scattering and refractive index detectors, Carbohydr. Polym. 49 (2002) 307–314.

[60] P. González, C. Medina, L. Famá, S. Goyanes, Biodegradable and non-retrogradable eco-films based on starch–glycerol with citric acid as crosslinking agent, Carbohydr. Polym. 138 (2016) 66–74.

[61] T.J. Gutiérrez, J. Suniaga, A. Monsalve, N.L. García, Influence of beet flour on the relationship surface-properties of edible and intelligent films made from native and modified plantain flour, Food Hydrocoll. 54 (2016) 234–244.

[62] S. Kalambur, S.S. Rizvi, Biodegradable and functionally superior starch-polyester nanocomposites from reactive extrusion, J. Appl. Polym. Sci. 96 (2005) 1072–1082.

[63] Y.X. Xu, K.M. Kim, M.A. Hanna, D. Nag, Chitosan-starch composite film: preparation and characterization, Ind. Crop. Prod. 21 (2005) 185–192.

[64] V.A. Pereira, I.N.Q. de Arruda, R. Stefani, Active chitosan/PVA films with anthocyanins from *Brassica oleraceae* (red cabbage) as time-temperature indicators for application in intelligent food packaging, Food Hydrocoll. 43 (2015) 180–188.

[65] S. Mathew, M. Brahmakumar, T.E. Abraham, Microstructural imaging and characterization of the mechanical, chemical, thermal, and swelling properties of starch–chitosan blend films, Biopolymers 82 (2006) 176–187.

[66] L.C.B. Reis, C.O. de Souza, J.B.A. da Silva, A.C. Martins, I.L. Nunes, J.I. Druzian, Active biocomposites of cassava starch: the effect of yerba mate extract and mango pulp as antioxidant additives on the properties and the stability of a packaged product, Food Bioprod. Process. 94 (2014) 382–391.

[67] R. Kizil, J. Irudayaraj, K. Seetharaman, Characterization of irradiated starches by using FT-Raman and FTIR spectroscopy, J. Agric. Food Chem. 50 (2002) 3912–3918.

[68] C.A. Romero-Bastidas, L.A. Bello-Pérez, M.A. García, M.N. Martino, J. Solorza-Feria, N.E. Zaritzky, Physicochemical and microstructural characterization of films prepared by thermal and cold gelatinization from non-conventional sources of starches, Carbohydr. Polym. 60 (2005) 235–244.

[69] J.M. Raquez, Y. Nabar, M. Srinivasan, B.Y. Shin, R. Narayan, P. Dubois, Maleated thermoplastic starch by reactive extrusion, Carbohydr. Polym. 74 (2008) 159–169.

[70] F.M. Pelissari, M.M. Andrade-Mahecha, P.J. do Amaral Sobral, F.C. Menegalli, Comparative study on the properties of flour and starch films of plantain bananas (*Musa paradisiaca*), Food Hydrocoll. 30 (2013) 681–690.

[71] M.A. García, M.N. Martino, N.E. Zaritzky, Lipid addition to improve barrier properties of edible starch-based films and coatings, J. Food Sci. 65 (2000) 941–944.

[72] A. García, M.N. Martino, N.E. Zaritzky, Microstructural characterization of plasticized starch-based films, Starch-Stärke 52 (2000) 118–124.

[73] S. Mali, M.V.E. Grossmann, M.A. Garcia, M.N. Martino, N.E. Zaritzky, Microstructural characterization of yam starch films, Carbohydr. Polym. 50 (2002) 379–386.

[74] M. Mitrus, Glass transition temperature of thermoplastic starches, Int. Agrophys. 19 (2005) 237–241.

[75] J. Bonilla, E. Fortunati, L. Atarés, A. Chiralt, J.M. Kenny, Physical, structural and antimicrobial properties of poly vinyl alcohol-chitosan biodegradable films, Food Hydrocoll. 35 (2014) 463–470.

[76] D. Schlemmer, E.R. De Oliveira, M.A. Sales, Polystyrene/thermoplastic starch blends with different plasticizers, J. Therm. Anal. Calorim. 87 (2007) 635–638.

[77] H.F. Zobel, Starch granule structure, in: R.J. Alexander, H.F. Zobel (Eds.), Developments in Carbohydrate Chemistry, The American Association of Cereal Chemists, St. Paul, MN 1994, pp. 1–36.

[78] I.A. Farhat, T. Oguntona, R.J. Neale, Characterisation of starches from West Africa ymas, J. Sci. Food Agric. 79 (1999) 2105–2112.

[79] L. Manzocco, M.C. Nicoli, T. Labuza, Study of bread staling by X-ray diffraction analysis, Ital. Food Technol. XII (2003) 17–23.

[80] C.A. Osella, H.D. Sánchez, C.R. Carrara, M.A. de la Torre, M.P. Buera, Water redistribution and structural changes of starch during storage of a gluten-free bread, Starch-Stärke 57 (2005) 208–216.

[81] P. Chang, P.B. Chea, C.C. Seow, Plasticizing–antiplasticizing effects of water on physical properties of cassava starch films in the glassy state, J. Food Sci. 65 (2000) 445–451.

[82] G. Hu, J. Chen, J. Gao, Preparation and characteristics of oxidized potato starch films, Carbohydr. Polym. 76 (2009) 291–298.

[83] M.S. Tapia, E. Pérez, P.E. Rodríguez, R. Guzmán, M.N. Ducamp-Collin, T. Tran, A. Rolland-Sabaté, Some properties of starch and starch edible films from sub-utilized roots and tubers from the Venezuelan Amazons, J. Cell. Plast. 48 (2012) 526–544.

[84] E. Pérez, X. Segovia, M.A. Tapia, M. Schroeder, Native and cross-linked modified *Dioscorea trifida* (cush-cush yam) starches as bio-matrices for edible films, J. Cell. Plast. 48 (2012) 545–556.

[85] D.D.S. Rosa, T.C. Rodrigues, C.D. Graças Fassina Guedes, M.R. Calil, Effect of thermal aging on the biodegradation of PCL, PHB-V, and their blends with starch in soil compost, J. Appl. Polym. Sci. 89 (2003) 3539–3546.

[86] E. Corradini, L.H.C. Mattoso, C.G.F. Guedes, D.S. Rosa, Mechanical, thermal and morphological properties of poly(ε-caprolactone)/zein blends, Polym. Adv. Technol. 15 (2004) 340–345.

[87] Y.V. García-Tejeda, C. López-González, J.P. Pérez-Orozco, R. Rendón-Villalobos, A. Jiménez-Pérez, E. Flores-Huicochea, J. Solorza-Feria, C.A. Bastida, Physicochemical and mechanical properties of extruded laminates from native and oxidized banana starch during storage, LWT Food Sci. Technol. 54 (2013) 447–455.

[88] S. Mali, M.V.E. Grossmann, M.A. García, M.N. Martino, N.E. Zaritzky, Effects of controlled storage on thermal, mechanical and barrier properties of plasticized films from different starch sources, J. Food Eng. 75 (2006) 453–460.

[89] T.J. Gutiérrez, M.S. Tapia, E. Pérez, L. Famá, Structural and mechanical properties of edible films made from native and modified cush-cush yam and cassava starch, Food Hydrocoll. 45 (2015) 211–217.

[90] T.J. Gutiérrez, R. Guzmán, C. Medina, L. Famá, Effect of beet flour on films made from biological macromolecules: Native and modified plantain flour, Int. J. Biol. Macromol. 82 (2016) 395–403.